Finite element modeling of offshore anchor piles under mooring forces

Mohamed I. Ramadan, Stephen D. Butt & Radu Popescu
Faculty of Engineering – Memorial University of Newfoundland, St. John's, NL, Canada

ABSTRACT
Offshore anchor piles are seafloor moorings that keep the position of Floating Production Storage Offloading vessels (FPSOs) during the harsh environment. These piles are usually subjected to a wide range of monotonic and cyclic lateral to oblique pull forces. In this paper, a 3D finite element model has been established to study the soil-pile interaction behavior under mooring forces. Mohr-Coulomb plastic model has been used to model the soil. The model has been validated based on existing experimental models of laterally and axially pullout loaded piles. After validating the model, oblique pull forces have been applied to study the pile behaviour under different loading angles. The obtained results have been compared to some available theoretical models in the literature.

RÉSUMÉ
Les piles d'ancrage en mer sont des amarrages sous-marin qui gardent la position des navires de débarquement de stockage de production de flottement (FPSOs) dans les environnements dur. Ces piles sont habituellement soumises aux forces de traction obliques, monotonique et cyclique. En ce document, un modèle d'élément fini 3D a été établi pour étudier l'interaction de sol-pile sous des forces d'amarrage. Le Mohr-Coulomb modèle plastique a été utilisé pour modeler le sol. Le modèle a été validé a basé sur des données expérimentales existantes pour piles chargées latéralement et axialement. Après validation du modèle, forces inclinées de traction ont été appliquées pour étudier le comportement de pile sous différents angles de chargement. Les résultats ont été comparés à quelques modèles théoriques disponibles dans la litérature.

1 INTRODUCTION

It has only been in the latter half of the 20th century that full recognition has been given to the oceans and their sediments as a major source of mineral wealth, both hard minerals and petroleum. Offshore oil and gas now supply almost one third of the world's energy needs. Because of the tremendous economic importance of offshore oil and gas and the concentrated development of technology for their exploitation, much of the recent marine construction practice has been devoted to the installation of facilities to serve the needs of the petroleum industry (Gerwick 2000).

In deep water, fixed offshore platforms are not economical due to the large amount of steel needed in constructing the supporting frame. Therefore, floating offshore structures became the economic alternative in deep waters. Floating structures are structures which are intended to remain floating throughout their service life. One of these floating structures that is widely used at the Grand Bank, Off Newfoundland, is Floating Production Storage Offloading vessels (FPSOs). FPSOs are widely used in offshore oil and gas industry in harsh environments at the Grand Banks, in water depths ranging from 80 to 200 m. They are kept on position using seafloor moorings which are commonly secured using anchor piles as shown in Figure 1. The anchor line, usually a shot of chain at this location, as shown in Figure 2, can lead from the top or from a point a few meters down the pile. The anchor pile resists pullout by a combination of bending plus passive resistance and skin friction shear.

Correctly designed anchor piles should transfer the environmental loads on the floating platforms to the seabed safely. In-service, these anchor piles are subjected to a wide range of monotonic and cyclic lateral to oblique pull forces. The large cyclic forces applied during extreme storm will tend to govern the design. The design of these anchor piles has not been codified as jacket piles which are widely used for fixed offshore platforms (Bhattacharya et. al. 2006). Also, both piles are different in geometry and applied loads. While jacket piles are fixed-head and axially loaded (compression/tension), anchor piles are free-head and incline loaded (close to lateral) piles. It is important to remember that the parameters for the lateral design of jacket piles are derived from lateral pile load tests on small diameter piles. The controlling design loads for jacket piles are usually the axial compressive and tensile loads, rather than the cyclic lateral loads. In contrast, the axial loads on FPSO piles are always tensile, and the lateral loads are much larger compared to the axial load. Therefore, the design of these anchor piles should not be the same as the jacket piles and there is extensive need to develop an accepted design method for this type of piles.

2 PREVIOUS RESEARCH

There is relatively limited experimental information on anchor piles or piles subjected to oblique pull loads. Due to the greater complexity of the response mechanism of an obliquely loaded anchor pile, this problem has received very little attention. The analyses proposed have made very crude assumptions which may invalidate their applicability to full scale. Most of the research done in this area was for lateral or tension loads on the piles. The effect of horizontal and vertical components of applied load has been assumed to be uncoupled (Hesar, 1991). Some of the existing theoretical models are semi-empirical based on 1g experimental tests as (Yoshimi 1964), (Broms 1965), (Das et. al., 1976), (Chattopadhyay and Pise 1986), (Ismael 1989), and (Jamnejad and Hesar 1995).

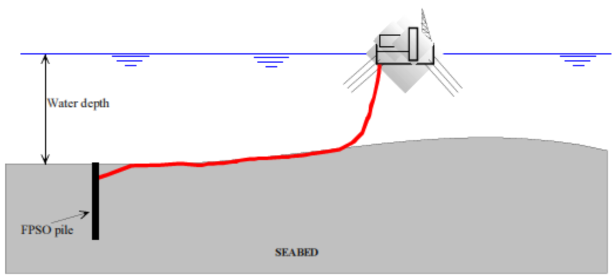

Figure 1. Schematic diagram of an FPSO and the anchoring system, (after Bhattacharya et. al. 2006)

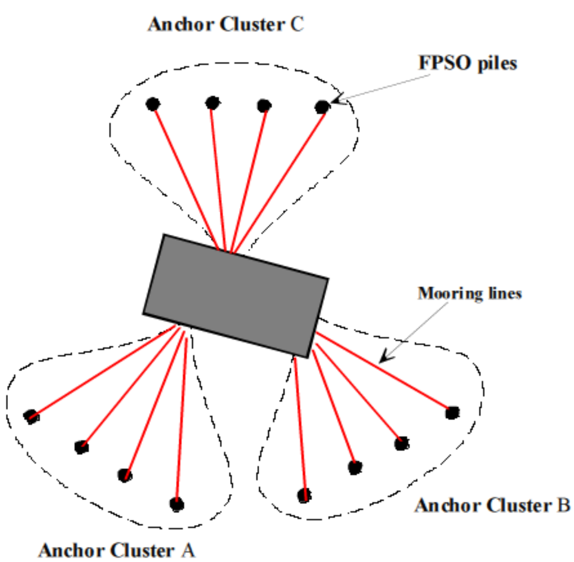

Figure 2. Schematic diagram of the anchoring system, (after Bhattacharya et. al. 2006)

Das, et. al. (1976) conducted some pullout tests on model rough rigid piles embedded in sand with angle of friction 31˚. To predict the oblique uplift capacity of rigid piles, they used the analysis suggested by Meyerhof (1973) for rigid vertical anchors with enlarged base:

$$\frac{Q_{u\theta}\cos\theta}{Q_{uv}} + \left(\frac{Q_{u\theta}\sin\theta}{Q_{uH}}\right)^2 = 1 \qquad [1]$$

where Q_{uv} and Q_{uH} are the ultimate resistance under tension (θ = 0˚) and lateral (θ = 90˚) loading as suggested by (Das et. al. 1976) and (Broms 1965) respectively. Chattopadhyay and Pise (1986) proposed a semi-empirical theoretical expression to evaluate the ultimate resistance of a pile embedded in sand, under oblique pull based on the experimental results. It takes into account the effects of the angle of inclination of the pull, the ultimate vertical uplift capacity and ultimate lateral resistance of the pile. In their expression, the net ultimate resistance P_θ has been predicted in terms of $\alpha = P_u/P_L$; (P_U is the ultimate uplift pile capacity, and P_L is the ultimate lateral pile capacity) and θ (angle of load inclination with vertical). After making several trial attempts for rigid and flexible piles with rough and smooth surface, the following relationship was identified:

$$\frac{P_\theta}{P_u} = \cos^2\theta \exp\left[-\left(\frac{1-\theta/90}{1+\theta/90}\right)\right] + \frac{\sin\theta}{\alpha}\exp\left[-\left(\frac{1-((90-\theta)/45)}{1+((90-\theta)/45)}\right)\right] \qquad [2]$$

As indicated by Altaee and Fellenius (1994), the dilation of the sand occurring at low confining stress -shallow depth- increases the lateral soil pressure against the pile. So, field tests using a small scale pile (Leshukov 1975 and Ismael 1989) will only eliminate the boundary conditions problem in the laboratory test, but the physical modeling issue will not be controlled and therefore their results cannot correctly reproduce the real behavior of the prototype scale piles under mooring forces for sandy soil. In addition, with the exception of Chattopadhyay and Pise (1986) and Jamnejad and Hesar (1995), no account has been taken of the flexibility of the anchor pile. Other models are based on the net uplift and the ultimate lateral capacity of the pile, whichever is smaller, as reported by Poulos and Davis (1980) and neglected the interaction between horizontal and vertical pull forces on the pile. Abdel-Rahman and Achmus (2006) and Achmus et. al. (2007) did a numerical analysis to study the interaction between horizontal and vertical loads for offshore piles. They suggested that this interaction must be considered in the determination of axial displacements under tension loading and thus in the serviceability design. However, the effect of cyclic loading on the interaction behavior should be investigated. Although the horizontal capacity is little affected by the tension capacity under monotonic loads, it is necessary to check against the tension failure, as skin friction will be reduced in the upper part of the pile due to the gap formation surrounding the pile during repeated cyclic loading. Therefore there is a need to do experimental research to study the behavior of this interaction under monotonic and cyclic loads.

The presented work aims at identifying the behavior and capacity of anchor piles used for anchoring offshore floating structures in saturated dense sand which is typical in the Grand Bank, offshore Newfoundland. Finite element method has been used to study the behavior of steel pipe anchor piles in saturated dense sand under mooring forces. A 3D model was established under different conditions of loading angles with horizontal θ, considering the soil-pile interaction. As both lateral and tension loading are the main loading conditions widely studied by the researchers, both cases have been examined to calibrate the model based on the available expressions for lateral and tension capacity suggested in the literature. In the next sections we will describe first the behavior of offshore piles under lateral and tension loading then describe oblique loading conditions.

3 BEHAVIOR OF OFFSHORE PILES UNDER TENSION LOADING

The most important factor that controls the tension behavior of driven piles is the shaft friction or the interaction of soil and pile wall in the transmission of forces from one to the other through the contact surface or interface. Many attempts had been made to predict the shaft friction along the pile experimentally and theoretically (Randolph et. al. 2005). The current API (2000) design guidelines adopt a conventional design approach for shaft friction is expressed as:

$$\tau_f = K\sigma_{vo} \tan \delta_f \qquad [3]$$

where; σ_{vo} is the initial soil vertical effective stress, δ_f is the interface friction angle, and limiting values of (τ_f) are varying with soil type and density. The lateral earth pressure coefficient (K) is recommended as 0.5 to 0.7 for open-ended piles loaded in tension, with the lower end applying to loose deposits and the upper end for dense conditions (Randolph 2003).

Adoption of a constant (K) value with depth in Equation 3, together with a limiting value for (τ_f) is not consistent with data from field tests. Extensive research has been done to investigate the shaft friction profile along the pile length due to the pile driving. Lehane et al. (1993), Jardine and Chow (1996), Jardine et al. (1998), White and Lehane (2004) and Schneider and Lehane (2005) illustrated the phenomenon of 'friction degradation' with profiles of shaft friction. Lehane et al. (1993) measured the shear stress in three instrument clusters at different distances (h) from the tip of a pile 6 m long and 0.1 m in diameter, as it is jacked into the ground. Comparison of the profiles from the instrument clusters at h/d = 4 and h/d = 25 shows that the friction measured at the latter position is generally less than 50% of that measured close to the pile tip, as shown in Figure 3. The value of K then reduces with distance, h, from the pile tip. The modified version of Equation 3 as confirmed by Lehane et al. (1993) is a function of the radial stress after installation and subsequent stress equalization (σ'_{rc}), the change in radial stress during the loading stress path ($\Delta\sigma'_{rd}$), and the interface friction angle(δ_f):

$$\tau_f = (\sigma'_{rc} + \Delta\sigma'_{rd}) \tan \delta_f = \sigma'_{rf} \tan \delta_f \qquad [4]$$

The value of ($\Delta\sigma'_{rd}$) is relatively small for pile diameters greater than about 300mm in siliceous sands as discussed by Lehane and Jardine (1994) and hence the radial effective stress at peak friction (σ'_{rf}) may be considered equivalent to (σ'_{rc}) for offshore piles. Schneider and Lehane (2005) worked out a correlation for the Imperial college design method (ICP-05) and Furgo design method (Furgo 2004). Their proposed formulation related the shaft friction to the cone penetration test (CPT) tip resistance. In their correlation they considered many factors including the (i) level of soil displacement imposed during installation, (ii) nature and method of pile installation (jacking/driving) (iii) dilation at the sand-pile interface, (iv) interface friction angle, (δ_f), (v) direction of loading (compression/tension), and (vi) elapsed time between installation and load testing. Taking these considerations into account and the need to reduce the number of empirical parameters because of the shortage of experimental data, the following simplified formula was given:

$$\sigma'_{rc} = 0.03 q_c (f/f_c)(D^*/D)^{0.6} \left[\max[(h/D), 2]\right]^{0.5} \qquad [5]$$

where; q_c is the cone penetration resistance and (f/f_c) ratio of 1.0 and 0.75 was assumed for compression and tension loading respectively.

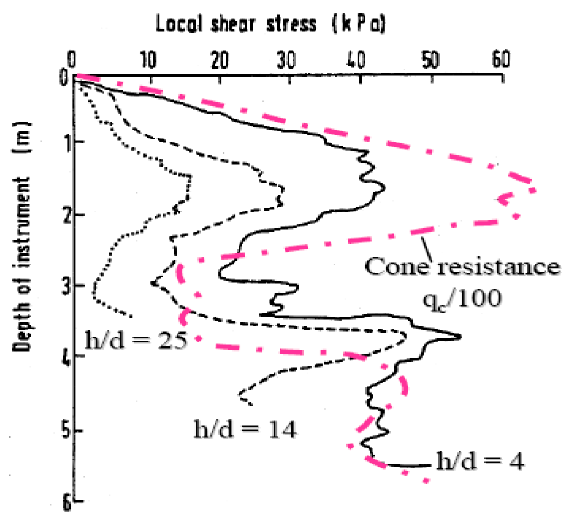

Figure 3. Measured profiles of shaft friction on a pile jacked into sand, (after Randolph 2003)

4 BEHAVIOR OF PILES UNDER LATERAL LOADING

The most widely used method in analyzing laterally loaded piles is the so called "p-y" method. In "p-y" method the soil is modelled by non-linear springs in which the soil reaction (P) at a given depth is undertaken by the spring and is a function of the lateral pile displacement (Y).

Many "p-y" curves have been established based on field or laboratory tests. One of the well known and widely used "p-y" curve for sand is the hyperbolic tangent function that has also been recommended in the form as indicated by API (2000). This formulation is non-linear and in the absence of more definitive information may be approximated at any specific depth "*z*", by the following expression:

$$p = Ap_u \tanh \frac{kz}{Ap_u} y \qquad [5]$$

where; A is a factor to account for cyclic or static loading condition, k is the initial modulus of sub-grade reaction (kN/m^3) determined as a function of the angle of internal friction, ϕ, and p_u is the ultimate pressure at depth *z* (kN/m).

However, to get the total ultimate lateral capacity of the piles, the "p-y" method needs to be implemented in software to get the pile head load deflection curve. Meyerhof (1995) offered solutions for laterally loaded rigid and flexible piles. According to Meyerhof's method, the relative stiffness of the pile to that of the soil (K_r) is given by:

$$K_r = \frac{E_p I_p}{E_s L^4} \qquad [6]$$

where E_pI_p is the flexural rigidity of the pile, with E_p is the Young's modulus of the pile, I_p is the moment of inertia of the pile cross section and E_s is the average horizontal soil modulus of elasticity along the embedded depth L of the pile.

For rigid piles in sand (K_r > 0.01), the ultimate load resistance (Q_{ur}) can be given as:

$$Q_{ur} = 0.12\,\gamma\, D\, L^2 K_{br} \le 0.4\, p_1\, D\, L \qquad [7]$$

where; γ is the soil unit weight, K_{br} is the resultant net soil pressure coefficient (Das 2005) and P_1 is the limit pressure obtained from pressure meter tests.

For flexible piles in sand, the ultimate lateral load (Q_{uf}) can be estimated from Equation 7 by substituting an effective length (L_e) for (L), where:

$$\frac{L_e}{L} = 1.65\, K_r^{0.12} \le 1 \qquad [8]$$

Zhang (2005) modified the above equation for rigid pile. He suggested the following equation to calculate the ultimate capacity of the rigid pile:

$$H_U = 0.3(\eta K^2_P + \zeta K \tan \delta)\, \gamma\, a\, D(2.7a - 1.7L) \qquad [9a]$$

where; e is the eccentricity of loading, L is the embedded length of the pile (see Figure 7), K_P is the passive earth pressure coefficient and equals to tan(45°+ ϕ/2), for circular pile $\eta = 0.8$ and $\zeta = 1$ and a is the depth to the point of rotation can be calculated as:

$$a = [-(0.567L + 2.7e) + (5.307L^2 + 7.29e^2 + 10.541eL)^{0.5}/2.1996 \qquad [9b]$$

5 NUMERICAL ANALYSIS

5.1 Model Parameters and Boundary Conditions

Numerical analysis was carried out using the ABAQUS 6.7 finite element analysis program (Hibbitt, et. al. 1998). The finite element mesh used in the analysis is shown in Figure 4. The elements used are 8-node continuum elements with porous properties for those elements modeling the soil. Due to the symmetric loading condition only a half-cylinder representing the soil and the pile was considered. The elements are biased towards the pile in order to get most of the data close to the pile. The limits of the mesh were at a diameter of 40m which is 20 times the pile diameter and 50m height, so the soil extends under the pile 5 times the pile diameter.

A steel pipe pile of 2m diameter, 0.10m wall thickness, and length to diameter ratio of 15 has been used in the analysis. The dimensions of this pile have been selected based on the in-service anchor piles at the Grand Bank (personal communication with Husky Energy) except for the wall thickness which is 0.05m for the in-service anchor piles. The material behavior of the pile was assumed to be linear elastic with Young's modulus (E) of 2.1×10^8 kN/m^2 and Poisson's ratio (ν) of 0.27 for steel.

The sand has been modeled as an elasto-plastic material with Mohr-Coulomb failure criterion. The angle of internal friction used in the analysis is for very dense sand for the Grand Banks (Thompson & Long 1989). Shear modulus has been calculated from the suggested equation by Baldi et al. (1989) as given by (Jardine et al. 1998):

$$G = q_c\left[A + B\eta - C\eta^2\right] \qquad [10a]$$

where; A, B and C are non-dimensional constants and η can be calculated as:

$$\eta = q_c \Big/ \sqrt{P_a \sigma_{vo}} \qquad [10b]$$

where; P_a is the standard atmospheric pressure.

The cone penetration resistance in the present study has been assumed to be increasing linearly with depth and obtained from fitted data of cone penetration resistance obtained from centrifuge testing by Zhu (1998) in dry dense sand and by De Nicola and Randolph (1997) for saturated dense sand. It was found that $q_c = 2\ z$, where q_c is the cone penetration resistance in MPa and z is the sand depth in meter. This fitting formula is close to the one suggested by (Rosquoët et al. 2007) with $q_C = 3\ z$ for a dry dense sand in a centrifuge test. Assuming a Poisson's ratio of 0.3 for dense sand which is constant with depth, the soil Young's modulus E has been calculated and implemented in the Finite Element Model (FEM) as a nonlinear function given in Table 1. This value is similar to the one suggested by (Janbu 1963). The other sand properties that have been used in (FEM) are given in Table 1. The dilation angle, ψ has been calculated as (Rowe 1962):

$$\sin\psi = \frac{\sin\phi - \sin\phi_{cv}}{1 - \sin\phi\sin\phi_{cv}} \qquad [11]$$

where ϕ_{CV} is the soil critical state friction angle.

As for driven piles, the soil pile interaction has been modeled using contact elements. The shear stress between the surfaces in contact was limited by a maximum value $\tau_{max} = \mu p$, where p is the normal effective contact pressure, and μ is the friction coefficient = tan δ. A value of 0.7ϕ has been selected for δ based on the suggestions given by (Jardine et al. 1998) for offshore steel piles.

Table 1. Sand parameters used FEM.

Soil Parameter	Value
Saturated unit weight, γ (kN/m^3)	11
Young's modulus, E (kN/m^2)*	14700*(σ_m/100)$^{0.66}$
Poisson's ratio, ν	0.3
Peak angle of internal friction, ϕ	40˚
Critical state friction angle, ϕ_{CV}	32˚
Dilation angle, ψ	10˚
Cohesion, c (kN/m^2)	1.0

* σ_m= mean effective stress (in kPa).

In the finite element analysis, the first step was the geostatic step for the soil to apply the soil gravity. In the next step the pile and the contact elements have been activated and a prescribed displacement has been applied at the top side node of the pile at the symmetry plan. For tension loading the pile was pulled axially at the center. The prescribed displacement has been applied with different angles (θ) to horizontal. The angles included 0˚ (lateral loading), 15˚, 30˚, 45˚, 60˚, 90˚ (tension loading) to simulate the pile under mooring conditions. The angles 0˚, 60˚ and 90˚ are not the case of mooring conditions; however they have been studied to get the ultimate lateral and pullout pile capacity of the anchor pile and to get a full view of the behaviour of the pile under such loading conditions.

5.2 Effect of Pile Installation

The pile installation method has a major effect on the pile loading behaviour. For offshore driven piles as discussed before, the lateral stresses will increase in the soil in a limited zone adjacent to the pile. Equation 5 has been used to calculate the lateral stress profile along the pile length for the present study conditions, as shown in Figure 5. The soil model has been divided into layers. The lateral earth pressure coefficient (K) value calculated based on Figure 5 has been assigned to each layer. Although the increase in the lateral stress should be limited to a limited zone around the pile, it has been found, to simplify the model and due to the analysis cost, that increasing the lateral stress along the full width of the soil model has little effect on the results as the main increase in the lateral stresses is concentrated to the pile tip vicinity which will have a negligible movement for a flexible pile.

Many centrifuge test studies, as described by (Rosquoët et al. 2007), concluded that the pile installation method had no effect on the pile behaviour under lateral loading. However such effect is major under tension loading or when there is inclined pullout load at the pile head as will be discussed later.

5.3 Model Calibration

The FEM has been calibrated by three methods. First it has been calibrated under tension loading by comparing the ultimate capacity obtained from the FEM with that from Equations 4 and 5. The second method is by calibrating for the lateral loading and comparing the ultimate capacity from the FEM at a displacement of 10 % of the pile diameter (Hesar 1991) with Equation 7. Both results are shown in Figure 6. There is good agreement between the FEM results and the suggested equation in the literature.

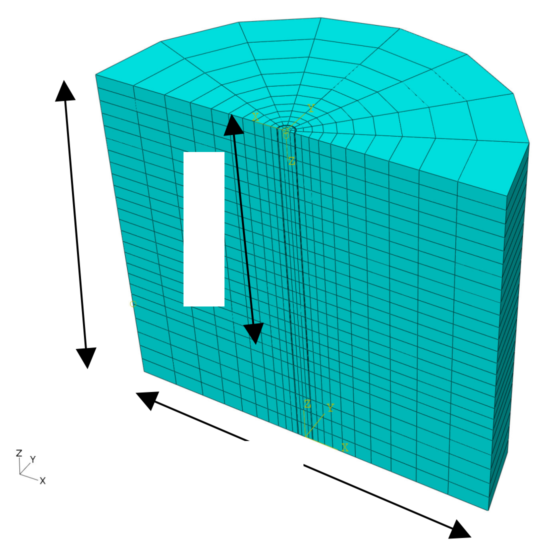

Figure 4. Finite Element Mesh for 2 m diameter and 30 m length steel pipe pile.

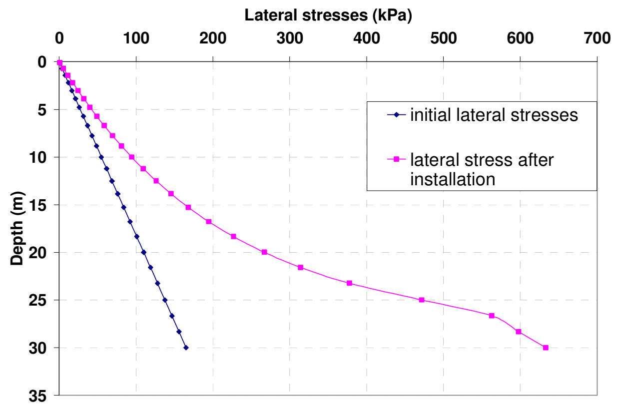

Figure 5. Lateral stress profile along the pile length before and after installation

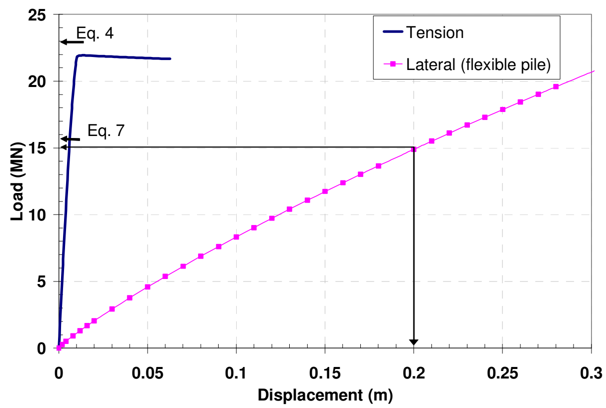

Figure 6. Comparison of FEM lateral and tension loading load-displacement curves to previous studies.

The third method to calibrate the model was to consider a rigid pile and compare the ultimate capacity of the pile to that from Equation 7 and 9. The rigid pile has been simulated in the FEM by increasing the pile Young's modulus to get a pile with high stiffness as in Equation 6 with K_r > 0.01. The pile used in this analysis has the same dimension as that used for the flexible pile. This method of calibrating the model has been used by Rosquoët et al. (2007) in their centrifuge test for closed ended pile. They tested a model pile with the same dimensions as the flexible pile but increased the pile stiffness by using a thick walled pile. The result for the present study calibration is shown in Figure 7. Again, as the previous case for the flexible pile, good agreement can be seen between FEM result and that by Equation 7 while Equation 9 predicts lower ultimate capacity. This difference from Equation 9 results from the simplification that was used for the model in implementing the increase in the lateral stress. As the increase in the lateral stresses was extended over the full width of the soil model, the high lateral stresses at the pile tip decreased the pile rotation and consequently increased the pile capacity. However, such conditions do not exist for the flexible pile case because of the negligible lateral movement at the pile tip.

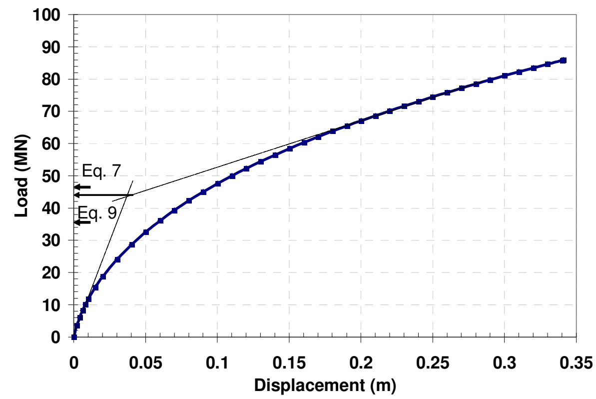

Figure 7. Comparison of FEM lateral loading load-displacement curve for rigid pile to previous studies.

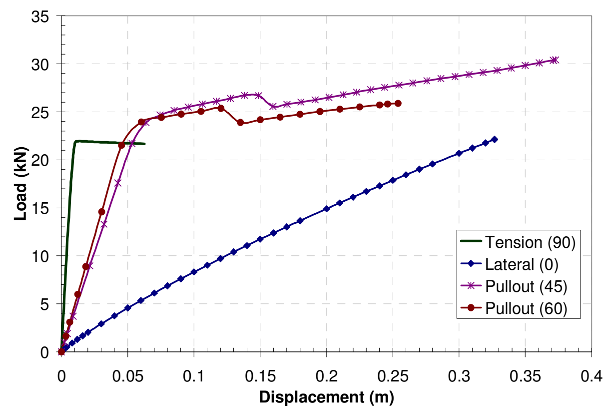

Figure 8. FEM load-displacement curves for loading angles 0˚, 45˚, 60˚ and 90˚.

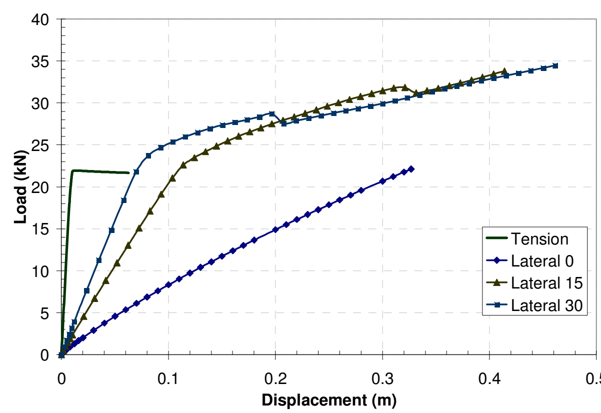

Figure 9. FEM load-displacement curves for loading angles 0˚, 15˚, 30˚ and 90˚.

6 RESULTS

After calibrating the model as discussed above, the oblique pullout loading was applied with angles 0˚ (lateral loading), 15˚, 30˚, 45˚, 60˚, 90˚ (tension loading). The load-displacement curves are shown in Figures 8 and 9. The ultimate load for the cases of angles 15˚, 30˚, 45˚, 60˚, 90˚ has been picked using the same method shown in Figure 7. For the lateral loading case, the ultimate load has been considered to be at 10 % of the pile diameter as mentioned by Hesar (1991) and shown in Figure 6. It should be mentioned that in all cases the plotted displacement is in the loading direction.

It can be observed that the oblique ultimate capacity is highly influenced by the tension load component. Even for the lowest inclination angle 15˚, the ultimate capacity is much higher than that for pure lateral loading. This is an important result which is different from the previous studies that suggest that the tension loading component can be neglected. This effect results from the pile installation effect which allows for much higher tension capacity than if the installation effect is neglected. This tension capacity can be compared to that obtained by Ramadan et al. (2009). In that paper, the same model was used without considering the effect of the pile installation. The pile tension capacity from Ramadan et al. (2009) study was 5 times lower than that obtained in the present study.

The ultimate pile capacity values of the different loading inclinations are given in Table 2. From these values, it can be seen that the ultimate capacity is increasing with decreasing load inclination angles. However, as the load is getting closer to lateral, the ultimate capacity decreases faster. So, there is a clear interaction between the lateral and tension loading even at angles close to lateral (i.e. 15˚).

Table 2. Ultimate Pile Capacity Calculated from FEM.

Inclination Angle	Ultimate Pile Capacity (Mpa)
0˚ (Lateral)	15
15˚ (Inclined Pullout)	25.8
30˚ (Inclined Pullout)	24.7
45˚ (Inclined Pullout)	24.4
60˚ (Inclined Pullout)	24
90˚ (Tension)	22

The lateral and tension pile capacity calculated from the FEM has been used in Equations 1 and 2 to calculate the ultimate pile capacity under the inclined load. Figure 10 shows a comparison of the FEM results and those from Equations 1 and 2. In the figure the ultimate pile capacity has been normalized to the tension capacity as suggested by Chattopadhyay and Pise (1986). It can be seen that both Equations 1 and 2 underestimate the ultimate pile capacity under inclined pullout loading, as compared to the FEM results obtained in the present study. The reasons for this under estimation include:

1. Both methods have been derived for piles driven in sand under low stresses. Such conditions will cause disturbance for a large zone around the pile resulting in low ultimate tension capacity and consequently lower ultimate inclined capacity.
2. Both equations are based on 1g test results. Because of the nonlinear stress-strain behavior and the dependence of the behavior on initial level of confining stress, small-scale physical modeling under 1g conditions has little relevance to the behavior of a full-scale prototype. The dilation of sand occurring at low confining stress (i.e. shallow depth) increases the lateral soil stress against the pile.
3. .Chattopadhyay and Pise (1986) did their tests for different pile flexibility and surface roughness. Therefore Equation 2 has been generalized for all cases.
4. Equation 1 was derived from tests on a rigid pile and it should not be used for offshore flexible piles.

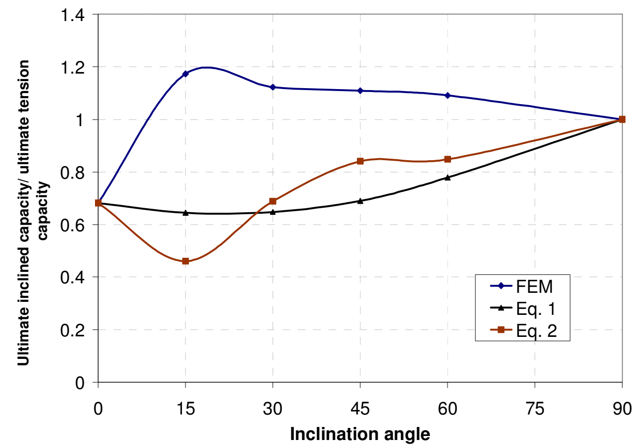

Figure 10. Comparison between the ultimate pile capacity results from FEM and previous studies.

CONCLUSION

From the present study and based upon the presented results and those in literature, it can be concluded that:

1. The behavior of piles under oblique pullout loading has not been studied as well as for lateral and tension loading.
2. All the previous research for oblique pullout loaded piles was conducted in a soil under low confining stresses and soil stiffness was not scaled (reduced) based on physical modeling scaling laws as the model dimensions.
3. Most of the previous studies on oblique pullout loaded piles were only for rigid piles. However, for offshore anchor piles, pile flexibility should be considered.
4. The pile installation method has a major effect on the pile behaviour under inclined pullout loading and should be considered in the analysis.
5. Although the FEM has been calibrated based on lateral and tension pile capacity available in the literature, experimental work, based on physical modeling scaling laws in geotechnical engineering (i.e. centrifuge test) is needed to validate the FEM and check other pile geometries and loading conditions such as cyclic loading which is the case for offshore anchor piles.

REFERENCES

Abdel-Rahman, K., and Achmus, M. 2006, Numerical modeling of the combined axial and lateral loading of vertical piles, Proceedings of the sixth European Conference in Geotechnical Engineering, Graz, Austria.

Achmus, M., Abdel-Rahman, K., and Wörden, F. 2007, Geotechnical design of piles supporting foundation structures for offshore wind energy converters, Proceedings of the seventeenth International Offshore and Polar Engineering Conference, Lisbon, Portugal.

Altaee, A., and Fellenius, B. 1994, Physical modeling in sand. *Canadian Geotechnical Journal* 31: 420-431.

API 2000. Recommended Practice for Planning, Designing and Constructing Fixed Offshore Platforms-Working Stress Design, RP2A-WSD 21st ed., American Petroleum Inst.

Bhattacharya, S., Carrington, T.M., and Aldridge, T.R. 2006, Design of FPSO piles against storm loading, Offshore Technology Conference, OTC 17861.

Broms 1965, Discussion of "Piles in cohesionless soil subject to oblique pull" by Y. Yoshimi. *Journal of the Soil Mechanics and Foundations Division*, ASCE 91: 199-205.

Chattopadhyay, B. C., and Pise, P. J. 1986, Ultimate resistance of vertical piles to oblique pulling load, Structural Engineering & Construction: Advances & Practice in East Asia & The Pacific, Proceedings of The First East Asian Conference on Structural Engineering & Construction, Bangkok, Thailand. 1: 1632-1641.

Das, B. M. Seeley, G. R. & Raghu, D. 1976, Uplift capacity of model piles under oblique loads. *Journal of the Geotechnical Engineering Division*, ASCE. 102: 1009-1013.

Das, B. M. 2005, *Principles of Foundation Engineering,* CL-Engineering, 5th edition.

De Nicola, A., and Randolph, M. F. 1997, Plugging behaviour of driven and jacked piles in sand. Géotechnique, 47(4):841 – 856.

Gerwick, B. 2000, *Construction of Marine and Offshore Structures*, CRC press.

Hibbitt Karlsson and Sorensen, Inc., 1998, *ABAQUS/Standard User Manuals*. (Pawtucket): Hibbitt. Karlsson & Sorensen, Inc, United States.

Hesar, M. 1991, *Behaviour of Pile-anchors Subjected to Monotonic and Cyclic Loading*, PhD Thesis, University of Sunderland, UK.

Ismael, Nabil F. 1989, Field tests on bored piles subject to axial and oblique pull. *Journal of Geotechnical Engineering* 115: 1588-1598.

Jamnejad, G. H., and Hesar, M. H. 1995, Stability of pile anchors in the offshore environment. Trans IMarE 107: 119–134.

Jardine, R.J. and Chow, F.C. 1996. *New Design Methods for Offshore Piles*, MTD Publication 96/103.

Jardine RJ, Overy RF, and Chow FC. 1998 Axial capacity of offshore piles in dense north sea sands. *J Geotechnical Geoenviron Eng*, ASCE;124(2):171–8.

Lehane, B.M., Jardine, R.J., Bond, A.J. and Frank, R. 1993, Mechanisms of shaft friction in sand from instrumented pile tests. *J. Geot. Eng. Div.*, ASCE, 119(1), 19-35.

Lehane, B.M. and Jardine, R.J. 1994. Shaft capacity of driven piles in sand: a new design approach. Proceedings, Behavior of Offshore Structures (BOSS):23 – 36.

Leshukov, M. R. 1975, Effect of oblique extracting forces on single piles, *Soil Mechanics and Foundation Engineering Journal* (English translation of Osnovaniya, Fundamenty i Mekhanika Gruntov). 12: 300-301.

Meyerhof, G. G. 1995, Standard penetration tests and pile behaviour under lateral loads in cohesionless soils, Canadian Geotechnical Journal, Vol. 32, 913-916.

Poulos and Davis 1980, *Pile foundation analysis and design*. New York: John Wiley & Sons.

Ramadan, M. I., Butt, S. D. and Popescu, R. 2009, Pipe piles under mooring forces, 17th International Conference of Soil Mechanics and Geotechnical Engineering, Alexandria, Egypt, 5-9 October.

Randolph, M.F. 2003, 43rd Rankine Lecture: Science and empiricism in pile foundation design. *Géotechnique*, 53(10), 847-875.

Randolph, M.F., Cassidy, M.J., Gourvenec, S. and Erbrich, C.J. 2005, Challenges of offshore geotechnical engineering, State of the Art paper. Proc. Int. Conf. on Soil Mech. and Found. Eng., Osaka.

Rosquoët, F., Thorel, L., Garnier, J., and Canepa, Y. 2007, Lateral Cyclic Loading of Sand-Installed Piles, *Soils and Foundations*, Vol. 47, No. 5, 821-832.

Rowe, P.W., 1962, The stress-dilatancy relation for static equilibrium of an assembly of particles in contact. Proc. of Royal. Society of London, 269(Series A), pp. 500-527.

Schneider, J.A., and Lehane, B.M. 2005, Correlations for shaft capacity of offshore piles in sand, International Symposium on Frontiers in Offshore Geotechnics, Perth, Australia, Taylor & Francis: 757-763.

Thompson, G. R. and Long, L. G. 1989. Hibernia geotechnical investigation and soil characterization. *Canadian Geotechnical Journal*. 26: 653-678.

White D.J. and Lehane B.M. 2004, Friction fatigue on displacement piles in sand. *Géotechnique*. 54(10):645-658.

Yoshimi, Y. 1964, Piles in cohesionless soil subject to oblique pull. Journal of the Soil Mechanics and Foundations Division, ASCE 90: 11-24.

Zhang, L., Silva, F. and Grismala, R. 2005, Ultimate lateral resistance to piles in cohesionless soils, *J. Geot. Eng. Div.*, ASCE, 131(1), 78-83.

Zhu, F., 1998, *Centrifuge Modelling and Numerical Analysis of Bearing Capacity of Ring Foundations on Sand*, PhD thesis, Memorial University of Newfoundland, St. John's, Canada.